Dictyostelium discoideum: cellular self-organization in an excitable biological medium

THOMAS HÖFER[1], JONATHAN A. SHERRATT[2] AND PHILIP K. MAINI[1]

[1] *Centre for Mathematical Biology, Mathematical Institute, University of Oxford, 24–29 St Giles', Oxford OX1 3LB, U.K.*
[2] *Nonlinear Systems Laboratory, Mathematics Institute, University of Warwick, Coventry CV4 7AL, U.K.*

SUMMARY

The dynamics which govern the establishment of pattern and form in multicellular organisms remain a key problem of developmental biology. We study this question in the case of morphogenesis during aggregation of the slime mould *Dictyostelium discoideum*. Here detailed experimental information allows the formulation of a mechanistic model in which the central element is the coupling of the previously much-studied intracellular cyclic AMP signalling with the chemotactic cell response in cyclic AMP gradients. Numerical simulations of the model show quantitatively how signal relay, chemotactic movement and adaptation orchestrate the collective modes of cell signalling and migration in the aggregating cell layer. The interaction of chemotaxis with the cyclic AMP excitation waves causes the initially homogeneous cell layer to become unstable towards the formation of a branching cell stream pattern with close cell–cell contacts as observed *in situ*. The evolving cell morphology in turn leads to a pattern of non-homogeneous excitability of the medium and thus feeds back into the cAMP dynamics. This feedback can explain the decrease in signalling period and propagation speed with time, as well as observations on the structure of the spiral wave core in this self-organized excitable medium.

1. INTRODUCTION

Under favourable environmental conditions, the cellular slime mould *Dictyostelium discoideum* exists in the form of single amoeboid cells that undergo division cycles. Starvation initiates a developmental programme that leads to cell aggregation and the formation of a primitive multicellular organism composed of typically about 10^4–10^5 cells. This organism passes through an intermediate motile phase (slug), before developing into a fruiting body. The comparative simplicity of multicellular morphogenesis has made *Dictyostelium* an attractive model system for the quantitative study of biological self-organization. Intercellular chemical signalling and chemotactically controlled cell movement play an essential role in this process (Devreotes 1989; Siegert & Weijer 1993). Mathematical models based on detailed experimental data successfully predict the collective patterns of cell–cell communication via cyclic adenosine 3′5′-monophosphate (cAMP) observed in cell suspensions (autonomous cAMP oscillations (Martiel & Goldbeter 1987; Tang & Othmer 1994)), during aggregation *in situ* (concentric and spiral waves of cAMP (Tyson *et al.* 1989; Monk & Othmer 1990)), and recently hypothesized in the moving slug (twisted cAMP scroll waves (Steinbock *et al.* 1993)). Briefly, aggregation-competent cells respond to stimulation by cAMP with a marked increase in cellular cAMP synthesis and subsequent secretion. This positive feedback is counteracted by a somewhat slower desensitization of the cAMP receptors by cAMP itself, which terminates the cell response. Both intra- and extracellular cAMP are degraded by phosphodiesterase, and cAMP returns to its resting level. The cAMP receptors resensitize, so the cell can be stimulated again. Diffusion of cAMP in the extracellular medium leads to the relay of the signal in space, which takes the form of the observed macroscopic cAMP waves. Thus the cAMP waves in *Dictyostelium* are a particular instance of wave patterns in so-called excitable media (Tyson & Murray 1989), which, first described in detail for the inorganic Belousov-Zhabotinskii reaction (see, for example, Field & Burger 1985), are widespread in living organisms (e.g. neural communication (Rinzel 1981), spread of excitation in heart muscle (Winfree 1987), intracellular calcium waves (Lechleiter *et al.* 1991)).

In contrast to the latter systems, the 'medium' in the case of *Dictyostelium* consists of cells which mechanically respond to the chemical signal via chemotaxis (Devreotes & Zigmond 1988; Newell & Liu 1992). This chemotactic cell response to cAMP has so far been neglected in the reaction–diffusion models of cAMP dynamics, and cells have been assumed to form a homogeneous stationary medium. Initially, this is a reasonable assumption, as the characteristic cell velocity, 20–30 μm min^{-1} (Siegert & Weijer 1993), is an order of magnitude smaller than the cAMP wave speed, *ca.* 300 μm min^{-1} (Alcantara & Monk 1974). Quite early in development, however, cell movement ceases to be simply slaved by the cAMP waves. This is shown in figure 1. Concentric and spiral waves of cAMP develop in the initially homogeneous layer of starved cells and induce periodic steps of cell movement towards the centre of the wave pattern (white bands in figure 1*a*). As aggregation proceeds, the development

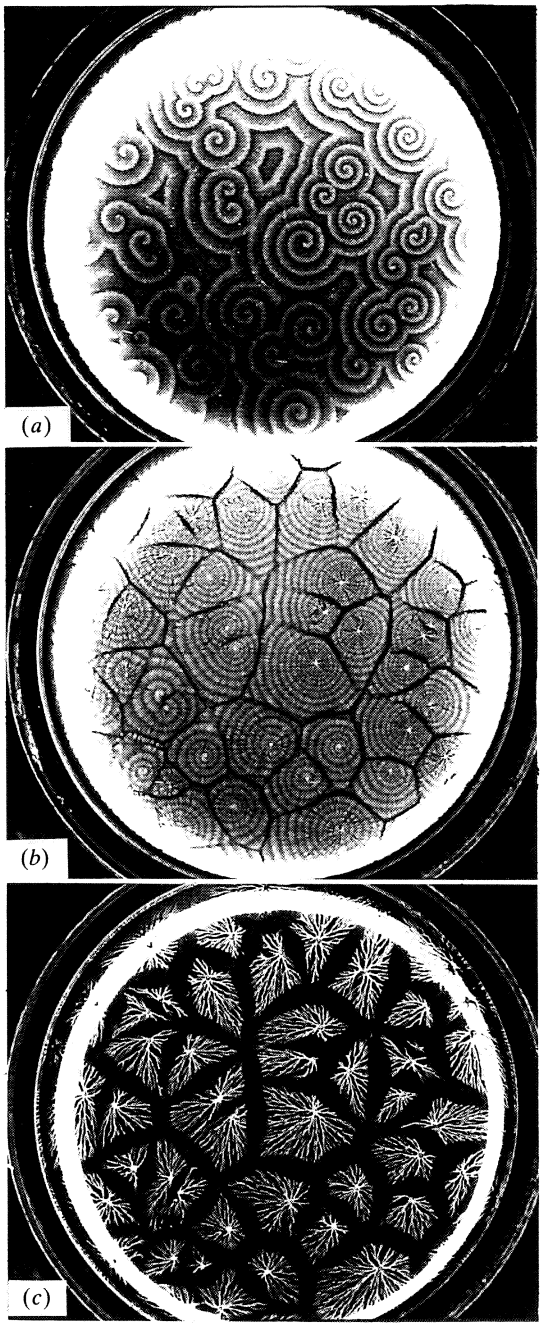

Figure 1. Aggregation of *Dictyostelium discoideum* on an agar plate showing the formation of spiral cAMP waves which induce (*a*) cell movement, (*b*) the onset of cell streaming, and (*c*) the development cell stream morphology in the whole aggregation territory; pictures taken *ca.* 30 min apart, the diameter of the dish is 5 cm. The position of the cAMP waves in (*a*) and (*b*) can be inferred from the different light-scattering responses of elongated (moving) and rounded (stationary) cells; amoebae elongate under the influence of the cAMP waves and form bright bands in the dark-field photograph. The strain used (strF NP377) shows particularly large streams due to the inability to form secondary aggregation centres. Photographs courtesy of P. C. Newell.

of a striking cellular morphology is observed: cells do not simply move straight to the aggregation centre, but form a pattern of branching cell streams (figure 1*b*, *c*). Cell streaming marks the onset of multicellularity: cell–cell contacts are established (Gerisch 1986) and trigger differential gene expression (Desbarats *et al.* 1994). Further aggregation to a mound takes place along these cell streams.

Here we investigate the mechanism of stream pattern formation. To obtain a quantitative description of the chemotactic behaviour of *Dictyostelium* amoebae, we use a previously proposed extension of the standard chemotaxis model for cell populations which includes a time-dependent adaptation response (Höfer *et al.* 1994). On this basis a reaction–diffusion–chemotaxis model is derived which accounts for the intrinsic coupling of cell movement with the cAMP signalling dynamics. This model exhibits a novel patterning scenario that predicts in quantitative detail the observed sequence of aggregation, as well as the effects of certain experimental manipulations on pattern formation.

2. THE MODEL

There has been much theoretical work on chemotaxis of both bacteria and eukaryotic cells (see, for example, Tranquillo *et al.* 1988; Maini *et al.* 1991; Stevens 1992; Sherratt *et al.* 1993). Computer simulations of *Dictyostelium* chemotaxis with discrete movement rules have been done by Parnas & Segel (1977), MacKay (1978), and Kessler & Levine (1993).

Different microscopic mechanisms of cell orientation lead to the same approximate expression for the cell flux, J, induced by the gradient, ∇u, of chemoattractant concentration, u, on the population level (Segel 1977; Alt 1980; Stevens 1992; Sherratt 1994),

$$J = \chi n \nabla u, \qquad (1)$$

where n denotes the cell density and χ the chemotactic coefficient. In the case of *Dictyostelium*, however, this flux expression results in a paradoxical conclusion (the 'chemotactic wave paradox' (Soll *et al.* 1993)). As the concentration profile of a single cAMP pulse is nearly symmetric (Tomchik & Devreotes 1981), according to equation (1), the chemotactic velocity profile under the influence of such a pulse would also be approximately symmetric. This would lead to cell movement opposite to the direction of wave propagation in the wavefront and with the wave in the waveback. As a consequence, amoebae would remain somewhat longer in the waveback than in the wavefront, and hence show a small net translocation in the direction of wave propagation, away from the aggregation centre. *In situ*, however, cells move only in the wavefront and remain more or less stationary in the waveback (Devreotes 1989; Siegert & Weijer 1993; Soll *et al.* 1993). Thus the chemotactic cell response cannot solely be determined by the local cAMP gradient. The explanation for this phenomenon is controversial; several different solutions have been suggested. One experimentally motivated hypothesis states that amoebae can orient, by some unspecified mechanism, in a spatial cAMP gradient only when it is accompanied by a temporal rise in cAMP concentration (Vicker *et al.* 1984). (Note that this hypothesis cannot simply rely on a temporal mechanism of the kind used by (considerably smaller and faster moving) bacteria. For a bacterial population, such a mechanism leads via appropriate averaging essentially to expression (1); see, for

example, Segel (1977).) This view is not confirmed by experiments which show persistent orientation and movement in shallow stationary cAMP gradients, although temporal changes of the cAMP profile seem to exert an additional influence on the motile cell behaviour (Fisher *et al.* 1989). Another hypothesis invokes the desensitization of the chemotactic machinery by the cAMP signal (Tomchik & Devreotes 1981), and thus introduces a temporal component in the chemotactic mechanism. Multiple molecular mechanisms of desensitization (adaptation) of the chemotactic signalling pathway by cAMP are known or hypothesized, with characteristic timescales ranging from about 10 s to 10 min (Van Haastert & Van der Heijden 1983; Devreotes & Zigmond 1988; Van Haastert *et al.* 1992). Inability to reorient quickly enough in the waveback due to the polarization of the motile machinery may also affect the behaviour in the natural cAMP waves.

Here we make the following assumptions: (i) in accordance with Fisher *et al.* (1989), amoebae are able to orient and move in spatial cAMP gradients (this can be achieved by spatial sampling of the concentration along a cell or pseudopod, or by temporal sampling over relatively short time intervals); and (ii) the presence of the chemotactic signal leads to a desensitization (in a wider sense) of the chemotactic machinery of the cell. This could either be a true desensitization of the signalling pathway (desensitized amoebae cannot 'feel' a cAMP gradient), or a 'desensitization' through the polarization of the motile machinery (amoebae can 'feel' a reversed gradient but are unable to reorient), or a combination of both. We can keep track of the ability of a cell to respond via the chemotactic coefficient, χ. It represents a combined measure of cellular sensitivity and motility, and hence should record the effect of desensitization upon exposure to the chemoattractant. A relatively simple way to implement this idea is to assume a direct biochemical modification of the chemotactic pathway, i.e. desensitization in the strict sense of the term. We take χ to depend on a sensitivity variable, v, which decreases as a result of binding of cAMP to the cell receptors (densensitization) and relaxes after cAMP withdrawal (resensitization). As a first approximation, the sensitivity variable is associated with the fraction of active cAMP receptors per cell. Receptor desensitization has been shown to occur with a characteristic time of about 1 min. This has been implemented by Martiel & Goldbeter (1987) in their model of cAMP signalling (and also, in a more recent model, Tang & Othmer (1994)), who derive the simple kinetic equation

$$\partial v/\partial t = \underbrace{-f_+(u)\,v}_{\text{desensitization}} + \underbrace{f_-(u)\,(1-v)}_{\text{resensitization}}, \tag{2}$$

where u denotes the cAMP concentration. We account for a response threshold of the cell by a sigmoid relation between χ and v, $\chi(v) = \chi_0 v^m/(A^m + v^m)$, $m > 1$. The conservation equation for the cell density then reads

$$\partial n/\partial t = \underbrace{\nabla\cdot[\mu(n)\,\nabla n]}_{\text{random migration}} - \underbrace{\nabla\cdot[\chi(v)\,n\nabla u]}_{\text{chemotaxis}}, \tag{3}$$

where we naturally focus on a two-dimensional domain, $\nabla \equiv (\partial/\partial x, \partial/\partial y)$. In addition to chemotaxis, random cell migration is included, with cell 'diffusivity' $\mu(n) = \mu_1 + \mu_2 N^4/(N^4 + n^4)$. This takes into account cell–cell adhesion, setting in at a critical cell density N. The magnitudes of the cell motility parameters μ and χ have been estimated experimentally for certain amoeboid leukocytes with a chemotactic response very similar to that of *Dictyostelium* (Tranquillo *et al.* 1988). The parameter values for the adaptation kinetics are taken from Martiel & Goldbeter (1987), who review experimental data (for numerical values of kinetic and motility parameters see figure 2). We have recently shown that this extension of the standard chemotaxis formalism equips amoebae with a short-term memory for experienced cAMP concentrations: cells move in wavefronts but remain stationary in wavebacks (Höfer *et al.* 1994). The modelling of desensitization via cell polarization would be somewhat more involved, as χ would then have to record previously experienced cAMP gradients which orient the motile machinery, rather than just the cAMP concentration. However, in the case of the natural aggregation waves, this should lead to the same result.

It is very likely that the complete picture of the chemotactic response is more complex. Even if the desensitization of the chemotactic signal transduction pathway is the main cause for the lack of response in the waveback, the adaptation kinetics of the adenylate cyclase pathway modelled and of the chemotactic pathway may not be identical, depending on which of the multiple desensitization mechanisms play the prominent role *in situ*. Nevertheless, the initial approach of (2)–(3) captures the essential features of *Dictyostelium* chemotaxis, and in particular has been shown to yield the correct timecourse of the cell velocity in response to the cAMP signal (see Höfer *et al.* (1994) for a discussion of the influence of the adaptation timescale on the movement response in a wave). As we shall see below, this will prove sufficient for a rather accurate description of pattern formation in the multicellular ensemble.

The evolution equation for the extracellular cAMP concentration reads (Martiel & Goldbeter 1987; Tyson *et al.* 1989):

$$\partial u/\partial t = \underbrace{\lambda\{\phi(n)\,g_+(u,v)}_{\text{synthesis}} - \underbrace{[\phi(n)+\delta]\,g_-(u)\}}_{\text{degradation}} + \underbrace{D\nabla^2 u}_{\text{diffusion}}. \tag{4}$$

For computational reasons we take somewhat simpler functional forms for the reaction rates $f_\pm$ and $g_\pm$ in equations (2) and (4) than those derived in Martiel & Goldbeter (1987) which nevertheless retain the important characteristics of the latter: $f_+ = k_+ u$, $f_- = k_-$, $g_+ = (bv + v^2)(a + u^2)/(1 + u^2)$, $g_- = du$.

Here, however, we account explicitly for the effect of local cell density on cAMP production and degradation via the factor $\phi(n)$ in equation (4). The derivation of equation (4) in Martiel & Goldbeter (1987) can be easily modified for the case of (slowly) varying cell density, and $\phi(n)$ naturally arises as the conversion factor of kinetic rates per cell into cAMP concentration

change in an extracellular volume element (see also Monk & Othmer 1990). Both cAMP production and degradation rates are influenced, as cells secrete cAMP and act as a source for extracellular phosphodiesterase. In addition we include some background activity of extracellular phosphodiesterase independent of cell density, $\delta g_{-}(u)$. The functional form of $\phi(n)$ is motivated as follows. An increase in cell density increases the local production and degradation rates per volume element, and it decreases locally the share of the extracellular volume in a volume element. These two effects combine to make $\phi(n)$ proportional to $n/(1-\rho n/n_c)$, where n_c and $1-\rho$ denote the cell density (number of cells per unit area) and the residual fraction of extracellular space in a confluent cell layer, respectively. Because of our two-dimensional formulation of the system, this would lead to a problem at the aggregation centre where cells start to pile, and hence n can exceed n_c. In this case, the denominator term, which accounts for exclusion of extracellar volume by the cells, should approach the constant value $1-\rho$ at high cell densities. We choose an empirical relation which can account for this:

$$\phi(n) = \frac{n}{[1-\rho n/(K+n)]},$$

with appropriate positive parameters ρ and K (in particular $0 < \rho < 1$). Note that cell density does not enter the rate expressions in equation (2), since it is written in terms of the fraction of active receptors per cell. However, as receptors are convected with cells, a convection term should be added to equation (2). This term can be shown to be of the form $-(J/n)\nabla v$ (Höfer *et al.* 1994). It turns out to be very small for the relevant parameter values, the reason essentially being the small ratio of cell velocity to wave speed, and therefore we neglect it.

The system (2)–(4) of nonlinear conservation equations for cell density, extracellular cAMP and fraction of active cAMP receptors per cell ('cellular sensitivity') was non-dimensionalized and solved numerically on a square domain of 5.3 mm × 5.3 mm, with zero-flux boundary conditions (see figure 2). The numerical algorithm uses a finite-difference approximation in space (five-point Laplacian, central differences for first derivatives); the resulting ordinary differential equation system is solved by Gear's method, allowing a relatively coarse spatial discretization of 71 × 71 meshpoints (Melgaard & Sincovec 1981). Tests with a finer grid (101 × 101 points) yielded practically identical results for spiral wave motion (both with fixed and moving cells) and the evolution of the cell pattern (see below). The scheme conserved the total cell number to within a maximum deviation of less than 2% for all results shown.

3. RESULTS AND DISCUSSION

Equations (2)–(4) constitute a minimal model of the aggregation process derived solely from individual cell properties. There are no global or long-range interactions present which could bias the system *a priori* towards a certain collective behaviour. Our extensive numerical simulations, however, reveal the rich patterning capacities of the model which can fully account for the basic phenomenology of *Dictyostelium* aggregation. The space–time evolution of cell distribution and cAMP signal in a representative simulation is shown in figure 2. The initially quiescent state of the cell layer is unstable towards the propagation of cAMP excitation waves. A rotating spiral wave pattern of cAMP develops from a disrupted wavefront, inducing cell movement towards the wave core. The interaction of the cAMP waves and cell chemotaxis then causes initial inhomogeneities in cell density to grow, and thus the cell distribution itself to be unstable. The dynamics select a particular patterning mode: cells form connected streams perpendicular to the cAMP wavefronts rather than isolated cell clusters. (The latter possibility is in fact realized in more primitive *Dictyostelium* species without chemoattractant waves. Species such as *D. minutum* and *D. lacteum* form small aggregation territories roughly on the scale of the characteristic wavelength of the emerging stream pattern in *D. discoideum*.) The spatial wavelength (width and spacing) of the stream pattern is independent of the spatial correlations of the initial random perturbations. This wavelength is the same throughout the aggregation territory, resulting in a branching pattern reminiscent of dendritic growth, as observed *in situ* (see figure 3 showing the power spectrum with a significant peak at the corresponding frequency.) We found that the streaming instability does not depend on the presence of the density-dependent diffusion term accounting for cell–cell adhesion. Streaming is also obtained with a constant cell diffusion coefficient. This agrees with the observation that cells treated with antibodies against cell adhesion molecules and adhesion-deficient mutants can still form somewhat rudimentary cell streams (Gerisch 1986). Thus it is the interaction of cAMP waves and chemotaxis which collects cells into streams that are then stabilized by cell–cell adhesion.

Preliminary linear analysis indicates how the stream pattern is forced by the repetitive cAMP pulses. Each pulse causes the pattern to grow by a small amount, which (partly) decays again between two pulses. In the course of many waves, overall growth of the pattern occurs, because the destabilizing effect of a cAMP pulse (determined jointly by cAMP production rate and chemotactic coefficient) overcomes the stabilizing influences of cell diffusion and cAMP degradation dominant between pulses. This instability mechanism explains why streams become visible first in the central region and 'grow' slowly outwards. Our analysis predicts a spatial wavelength of the stream pattern (corresponding to the fastest growing linear mode) and a temporal growth rate (the Floquet multiplier of this mode) that are in very good agreement with the numerical simulations and *in situ* observations, and also shows the relation of the streaming instability to the classical (non-oscillatory) chemotactic instability first discussed by Keller & Segel (1970) (Höfer *et al.* 1995).

The first ten or so waves (equivalent to spiral rotations: at a fixed point the rotating spiral appears as a sequence of cAMP pulses) are only locally distorted

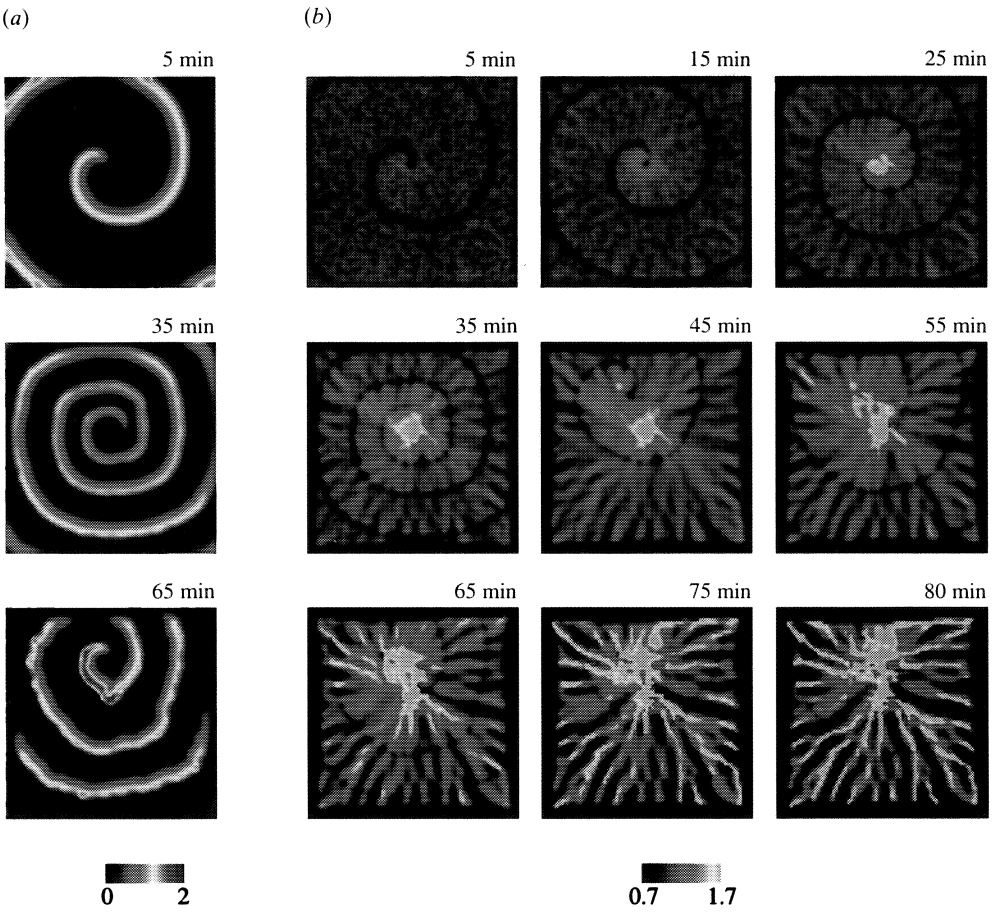

Figure 2. Spatio-temporal evolution (*a*) cAMP concentration, and (*b*) cell density in a representative computer simulation. The first (5–25 min), second (35–55 min) and third (65–80 min) rows in (*b*) roughly correspond to the aggregation stages shown in figure 1 (*a*), (*b*) and (*c*), respectively. The domain size is 5.3 mm × 5.3 mm, and 'snapshots' are taken at the times indicated. The model equations (2)–(4) were non-dimensionalized with characteristic reference values for all the variables: time unit 2.5 min, length unit 214 μm, cAMP concentration 5×10^{-7} M, average number of receptors per cell 10^6, reference cell density 1.5×10^4 cm^{-2}. For better resolution, cell densities greater than 1.7 and smaller than 0.7 are mapped to the respective colours for these values. Parameter values: $\lambda = 70.0$, $a = 0.014$, $b = 0.2$, $\rho = 0.7$, $K = 0.8$, $d = 0.0234$, $\delta = 0.11$, $k_+ = k_- = 2.5$, $\mu_1 = 0.003$, $\mu_2 = 0.0095$, $N = 1.2$, $\chi_0 = 0.5$, $A = 0.72$, and $m = 10.0$. The diffusivity of cAMP was assumed to be 75% of its value in water (Dworkin & Keller 1977), i.e. 18×10^3 μm^2 min^{-1}, yielding a non-dimensional value of 1. A random perturbation between −0.075 and 0.075 was added to the initial cell density (1.0) at every mesh point.

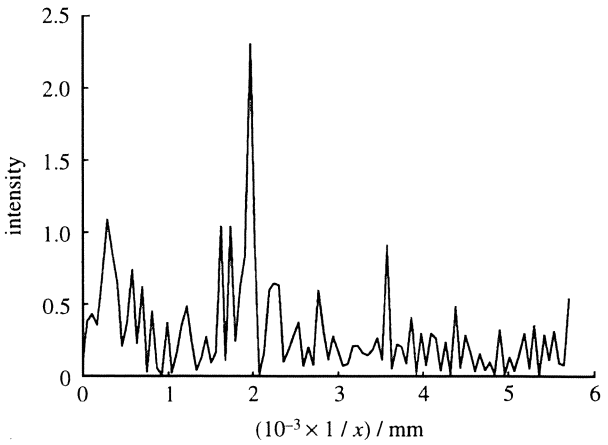

Figure 3. Power spectrum of the cell density distribution in simulation of figure 2, sampled on the curve defined by the isoconcentration contour $u = 0.5$ in the cAMP waveback at 25 min. The growth of a (small-amplitude) pattern with a dominant wavelength of *ca.* 510 μm is clearly visible.

by the inhomogeneities in cell density. After leaving the core region where the curvature effect decreases the wave speed notably (see below), each pulse travels with a constant velocity, and the global geometry of the spiral is retained. However, each pulse changes the propagation conditions for its successor by enhancing stream formation, and so we find systematic differences between consecutive waves. As signal propagation becomes focused along the developing cell streams, the signalling frequency increases while propagation velocity drops (figure 4; cf. also the decrease in the spatial period of the spirals in figures 1 and 2). This phenomenon is well known *in situ*. It has been attributed to speculative biochemical changes, which would have to be stimulated directly by the cAMP waves (Gross *et al.* 1974), and in the model would make parameters time dependent or necessitate the introduction of new variables. Here we reproduce the concomitant decrease in signalling period and wave speed with a simple set of assumptions and constant parameters. In our framework, this phenomenon is

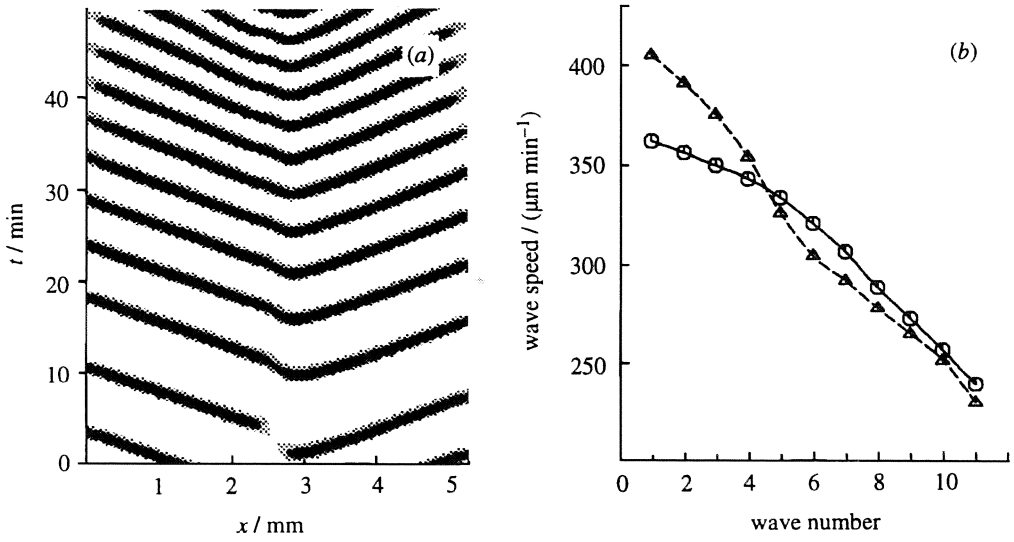

Figure 4. (*a*) Evolution of cAMP concentration in a spatial slice through the aggregation territory; (*b*) corresponding wave velocities (circles, solid line), compared with the experimental data in Gross *et al.* (1974), figure 3 (triangles, broken line). The spatial slice is taken parallel to the horizontal boundary, and 2.6 mm away from it. A fully developed spiral wave was used as initial condition (in 'control' integration with cell density fixed at 1.0 the spiral geometry and rotation frequency remain unchanged).

linked to wave speed dispersion, that is, the decrease of wave speed with decreasing wave period. Such a dispersion relation between propagation speed and period is a general property of excitable media, and is due to the existence of a relative refractory period of the excitable kinetics (Tyson & Keener 1988). In a homogeneous excitable medium, a spiral wave normally evolves, after an initial transient, to a stationary shape (in a coordinate system rotating with an appropriate constant velocity), and then stays at a certain point on the dispersion curve. In the present case, however, cell density slowly varies and increases in the centre of the pattern and along the outward growing streams. This corresponds to a local increase in excitability of the medium which causes the rotation frequency of the spiral to increase in the centre (the excitability of the cAMP kinetics is measured by the parameter λ and, for cell densities that are not too high, an increase in n is equivalent to an increase in λ). Increased rotation frequency in the central region implies that the surrounding medium is excited with a shorter period, and this in turn pushes it downwards on the dispersion curve towards a lower propagation speed. It should be noted that this mechanism does not actually depend on how the slow increase of excitability towards the aggregation centre is achieved. It is conceivable that biochemical modifications, which are forced by the cAMP waves and effectively increase λ, also play a role.

The *Dictyostelium* aggregation field is considered a classical example of an excitable medium. The above results clearly demonstrate that this system is considerably more complex than a 'generic' excitable medium such as the Belouzov-Zhabotinskii reaction. It not only exhibits anisotropic excitability in later aggregation stages, but it appears to be the first instance of a medium which self-organizes its excitability properties in the active (i.e. wave-propagating) state.

This is further emphasized by an observation concerning the structure of the core region. Experimental treatment of the aggregation field with caffeine causes the formation of cell loops rather than mounds in the centre of the wave patterns (Siegert & Weijer 1993). Caffeine is known to inhibit the adenylate cyclase pathway (Brenner & Thoms 1987). This results in a decreased excitability of the medium, which can be crudely reflected in the model by a decrease in the value of λ, clearly leading to the prediction of loop formation (figure 5*a*, *b*). Loop formation links another well-known property of spirals in excitable media, namely, the migration of the spiral tip, with the dynamics of cell movement. In general, the propagation velocity of a wave in an excitable medium depends not only on wave period (dispersion) but also on the curvature of the wavefront; one can derive the approximate relation $c(\kappa) = c_\infty - D\kappa$, where c, c_∞, κ and D denote the local wave speed, the speed of a plane wave, the local front curvature, and the diffusion coefficient of the propagator species, respectively (Tyson & Keener 1988; Mikhailov *et al.* 1994). This 'eikonal' equation implies that a wave cannot form a perfect spiral but has to terminate at a certain curvature, thereby creating a free tip which moves along a circular path, the so-called wave core (more complicated meandering of the tip can be observed in media with low excitability; see Mikhailov *et al.* (1994)). The radius of the wave core depends on the excitability of the medium (which enters the above dimensional form of the eikonal equation via c_∞). The typical core radius in *Dictyostelium* at the onset of aggregation has been estimated both from experiments (Foerster *et al.* 1990) and models (Tyson *et al.* 1989) to range between 100 μm and 300 μm. We find an initial value of about 290 μm for the simulations of figure 2 (figure 5*c*). As cells aggregate in the centre, a mound is usually formed, i.e. cell density increases also in the immediate core region, against the local chemotactic

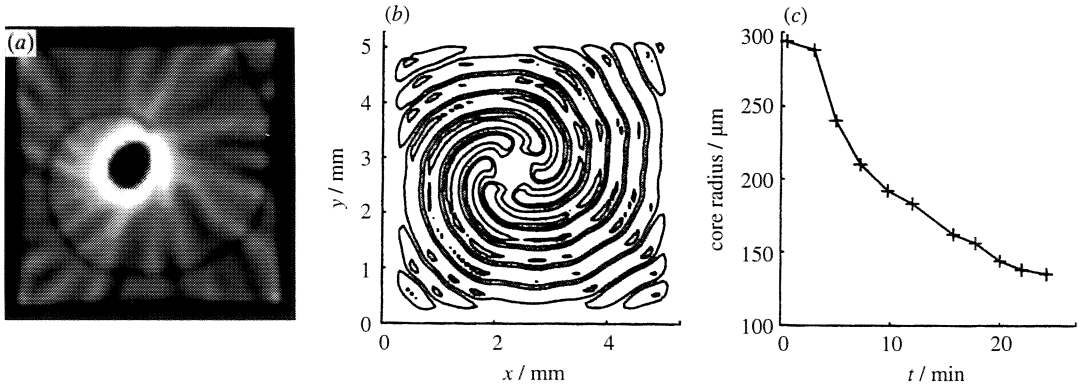

Figure 5. The formation of a cell loop: (*a*) cell density (grey scale ranging from 0.7 to 1.7) and (*b*) cAMP concentration (concentration contours 0.8 and 1.1, at six consecutive times *ca.* 1 min apart); parameters as in figure 2 except $\lambda = 55.0$, modelling caffeine treatment. The radius of the cAMP wave core is *ca.* 0.5 mm. In contrast, (*c*) shows the decrease in core radius in a simulation with $\lambda = 70.0$ as in figure 2. For estimating the core radius according to the definition given in Tyson & Keener (1988), the concentration contour $u = 0.9$ was used.

gradient. Random cell migration, the 'pushing' of incoming cells and cell–cell adhesion may contribute to this. As discussed above, increasing cell density (and *in situ* perhaps also biochemical modifications) leads to an increase of excitability in the centre with time and hence we find a continuous decrease of the core diameter in the model (cf. figure 5*c*). If the initial excitability is sufficiently low, however, the diameter of the core path is large enough for the core region to be depleted of cells by chemotaxis before aggregation can limit core migration, with random cell movement not being able to counteract this process. A stable ring of amoebae is then formed, and the spiral core becomes locked into the path prescribed by this ring. Cells rotate opposite to the direction of core migration around the ring (similar cell rotation also takes place in the growing mound). This explanation suggests that loops should occasionally be seen under normal conditions in regions with relatively low cell density. This is the case in the model, and 'spontaneous' loop formation can indeed be observed *in situ* (P. Newell, personal communication).

Thus, depending on the initial conditions, the model yields either a continuous decrease in core radius or the locking of core motion into a cell loop. Previous measurements of the core size have been performed at the onset of aggregation (Foerster *et al.* 1990); the model prediction of its decrease with time should in principle be testable experimentally.

4. CONCLUSIONS

Spatio-temporally controlled collective cell movement is a key element in many morphogenetic processes. For the specific and relatively simple case of *Dictyostelium* aggregation, our results demonstrate in mechanistic detail that cellular morphogenesis can be rationalized on a physico-chemical basis. The streaming instability gives rise to a standing wave pattern of cell streams, which formally is the type of pattern addressed by the standard Turing, chemotaxis and mechanochemical models (Murray 1989). However, we have gained direct insight into the underlying mechanisms for cell streaming which turn out to be very specific and different from the ones dealt with by these 'generic' models. In particular, we find that the character and polarity of the cell pattern is controlled by the dynamic chemical 'pre-pattern' of repetitive excitation waves. Thus our model establishes an interesting link between two hitherto quite distinct areas in the investigation of biological pattern formation, excitable media and (multicellular) morphogenesis. It supports the view of morphogenesis as a sequence of dynamical instabilities, creating successive patterns of increasing complexity. Interestingly, the desensitization–resensitization dynamics of chemotactic and adenylate cyclase pathways, which for the single cell could be interpreted as environmental adaptation, are a crucial element of pattern formation in the cellular ensemble.

Recent experimental work points to the central role of periodic cAMP signals and chemotaxis also in the subsequent 'tissue-like' stages of *Dictyostelium* morphogenesis. Both the mound and the slug stage are characterized by collective cell movement patterns which appear again to be organized by excitation waves, presumably carried by cAMP (Siegert & Weijer 1993; Siegert *et al.* 1994). In the slug, this leads to the migration of the cell mass as a whole, and to the sorting of differentiating cell types. Our results show that the dynamic interaction of biochemical signalling and cell mechanics is crucial for the understanding of pattern formation along this primitive route to multicellularity.

T.H. and P.K.M. thank P. C. Newell for stimulating discussions. T.H. acknowledges support from the Boehringer Ingelheim Fonds, the Engineering and Physical Sciences Research Council of Great Britain, and a Jowett Senior Scholarship at Balliol College, Oxford.

REFERENCES

Alcantara, F. & Monk, M. 1974 Signal propagation during aggregation in the slime mould *Dictyostelium discoideum*. *J. gen. Microbiol.* **85**, 321–334.

Alt, W. 1980 Biased random walk models for chemotaxis and related diffusion approximations. *J. math. Biol.* **9**, 147–177.

Brenner, M. & Thoms, S. 1984 Caffeine blocks activation of cyclic AMP synthesis in *Dictyostelium discoideum*. *Devl Biol.* **101**, 136–146.

Desbarats, L., Brar, S. K. & Sin, C.-H. 1994 Involvement of cell-cell adhesion in the expression of the cell cohesion molecule gp80 in *Dictyostelium discoideum*. *J. Cell Sci.* **107**, 1705–1712.

Devreotes, P. N. 1989 *Dictyostelium discoideum*: a model system for cell–cell interactions in development. *Science, Wash.* **245**, 1054–1059.

Devreotes, P. N. & Zigmond, S. H. 1988 Chemotaxis in eukaryotic cells: a focus on leukocytes and *Dictyostelium*. *A. Rev. Cell Biol* **4**, 649–686.

Dworkin, M. & Keller, K. H. 1977 Solubility and diffusion coefficient of adenosine 3′,5′ monophosphate. *J. biol. Chem.* **252**, 864–865.

Field, R. J. & Burger, M., (ed.) 1985 *Oscillations and travelling waves in chemical systems*. New York: Wiley.

Fisher, P. R., Merkl, R. & Gerisch, G. 1989 Quantitative analysis of cell motility and chemotaxis in *Dictyostelium discoideum* by using an image processing system and a novel chemotaxis chamber providing stationary chemical gradients. *J. Cell Biol.* **108**, 973–984.

Foerster, P., Müller, S. C & Hess, B. 1990 Curvature and spiral geometry in aggregation patterns of *Dictyostelium discoideum*. *Development* **109**, 11–16.

Gerisch, G. 1986 Interrelation of cell adhesion and differentiation in *Dictyostelium discoideum*. *J. Cell Sci.* **4** (Suppl.), 201–219.

Gross, J. D., Peacey, M. J. & Trevan, D. J. 1974 Signal emission and relay propagation during early aggregation in *Dictyostelium discoideum*. *J. Cell Sci.* **22**, 645–656.

Höfer, T., Maini, P. K., Sherratt, J. A., Chaplain, M. A. J., Chauvet, P., Metevier, D., Montes, P. C. & Murray, J. D. 1994 A resolution of the chemotactic wave paradox. *Appl. Math. Lett.* **7**, 1–5.

Höfer, T., Sherratt, J. A. & Maini, P. K. 1995 Cellular pattern formation during *Dictyostelium* aggregation. *Physica D.* (In the press.)

Keller, E. F. & Segel, L. E. 1970 Initiation of slime mold aggregation viewed as an instability. *J. theor. Biol.* **26**, 399–415.

Kessler, D. A. & Levine, H. 1993 Pattern formation in *Dictyostelium* via the dynamics of cooperative biological entities. *Phys. Rev. E* **48**, 4801–4804.

Lechleiter, J., Girard, S., Peralta, E. & Clapham, D. 1991 Spiral calcium wave propagation and annihilation in *Xenopus laevis* oocytes. *Science, Wash.* **252**, 123–126.

MacKay, S. A. 1978 Computer simulation of aggregation in *Dictyostelium discoideum*. *J. Cell Sci.* **33**, 1–16.

Maini, P. K., Myerscough, M. R., Winters, K. H. & Murray, J. D. 1991 Bifurcating spatially heterogeneous solutions in a chemotaxis model for biological pattern formation. *Bull. math. Biol.* **53**, 701–719.

Martiel, J.-L. & Goldbeter, A. 1987 A model based on receptor desensitization for cyclic AMP signaling in *Dictyostelium* cells. *Biophys. J.* **52**, 897–828.

Melgaard, D. K. & Sincovec, R. F. 1981 General software for two-dimensional nonlinear partial differential equations. *ACM Trans. Math. Softw.* **7**, 106–125.

Mikhailov, A. S., Davydov, V. A. & Zykov, V. S. 1994 Complex dynamics of spiral waves and motion of curves. *Physica D* **70**, 1–39.

Monk, P. B. & Othmer, H. G. 1990 Wave propagation in aggregation fields of the cellular slime mould *Dictyostelium discoideum*. *Proc. R. Soc. Lond.* B **240**, 555–589.

Murray, J. D. 1989 *Mathematical biology*. Berlin: Springer-Verlag.

Newell, P. C. & Liu, G. 1992 Streamer F mutants and chemotaxis of *Dictyostelium*. *BioEssays* **14**, 473–479.

Parnas, H. & Segel, L. A. 1977 Computer evidence concerning the chemotactic signal in *Dictyostelium discoideum*. *J. Cell Sci.* **25**, 191–204.

Rinzel, J. 1981 Models in neurobiology. In *Nonlinear phenomena in physics and biology* (ed. R. H. Enns, B. L. Jones, R. M. Miura. & S. S. Rangnekar), pp. 345–367. New York: Plenum, Press.

Segel, L. A. 1977 A theoretical study of receptor mechanisms in bacterial chemotaxis. *SIAM Jl appl. Math.* **32**, 653–665.

Sherratt, J. A. 1994 Chemotaxis and chemokinesis in eukaryotic cells: the Keller–Segel equations as an approximation to a detailed model. *Bull. math. Biol.* **56**, 129–146.

Sherratt, J. A., Sage, E. H. & Murray, J. D. 1993 Chemotactic control of eukaryotic cell movement: a new model. *J. theor. Biol.* **162**, 23–40.

Siegert, F. & Weijer, C. J. 1993 The role of periodic signals in the morphogenesis of *Dictyostelium discoideum*. In *Oscillations and morphogenesis* (ed. L. Rensing), pp. 133–152. New York: Marcel Dekker.

Siegert, F., Weijer, C. J., Nomura, A. & Miike, H. 1994 A gradient method for the quantitative analysis of cell movement and tissue flow and its application to the analysis of multicellular *Dictyostelium* development. *J. Cell Sci.* **107**, 97–104.

Soll, D. R., Wessels, D. & Sylvester, A. 1993 The motile behaviour of amoebae in the aggregation wave in *Dictyostelium discoideum*. In *Experimental and theoretical advances in biological pattern formation* (ed. H. G. Othmer, P. K. Maini & J. D. Murray), pp. 325–338. New York: Plenum, Press.

Steinbock, O., Siegert, F., Müller, S. C. & Weijer, C. J. 1993 Three-dimensional waves of excitation during *Dictyostelium* morphogenesis. *Proc. natn. Acad. Sci. U.S.A.* **90**, 7332–7335.

Stevens, A. 1992 Mathematical modeling and simulations of the aggregation of myxobacteria (chemotaxis equations as limit dynamics of a moderately interacting stochastic processes). Unpublished. PhD thesis, University of Heidelberg.

Tang, Y. & Othmer, H. G. 1994 A G-protein based model of adaptation in *Dictyostelium discoideum*. *Math. Biosci.* **120**, 25–76.

Tomchik, K. J. & Devreotes, P. N. 1981 Adenosine 3′,5′-monophosphate waves in *Dictyostelium discoideum*: a demonstration by isotope dilution-fluorography. *Science, Wash.* **212**, 443–446.

Tranquillo, R. T., Zigmond, S. H. & Lauffenburger, D. A. 1988 Measurement of the chemotaxis coefficient for human neutrophils in the under-agarose migration assay. *Cell Motil. Cytoskeleton* **11**, 1–15.

Tyson, J. J. & Keener, J. P. 1988 Singular perturbation theory of traveling waves in excitable media (a review). *Physica D* **32**, 327–361.

Tyson, J. J. & Murray, J. D. 1989 Cyclic AMP waves during aggregation of *Dictyostelium* amoebae. *Development* **106**, 421–426.

Tyson, J. J., Alexander, K. A., Manoranjan, V. S. & Murray, J. D. 1989 Spiral waves of cyclic AMP in a model of slime mold aggregation. *Physica D* **34**, 193–207.

Van Haastert, P. J. & Van der Heijden, P. R. 1983 Excitation, adaptation and deadaptation of the cAMP mediated cAMP response in *Dictyostelium discoideum*. *J. Cell Biol.* **96**, 347–353.

Van Haastert, P. J., Wang, M., Bominaar, A. A., Devreotes, P. N. & Schaap, P. 1992 cAMP-induced desensitization of surface cAMP receptors in *Dictyostelium*: different second messengers mediate receptor phosphorylation, loss of ligand binding, degradation of receptor, and reduction of receptor mRNA levels. *Molec. Biol. Cell* **3**, 603–612.

Vicker, M. G., Schill, W. & Drescher, K. 1984 Chemoattraction and chemotaxis in *Dictyostelium discoideum*: myxamoeba cannot read spatial gradients of cyclic adenosine monophosphate. *J. Cell Biol.* **94**, 2204–2214.

Winfree, A. T. 1987 *When time breaks down*. Princeton University Press.

Received 27 October 1994; accepted 7 December 1994